STAT1-HDAC4 signaling induces epithelial-mesenchymal transition and sphere formation of cancer cells overexpressing the oncogene, *CUG2*

SIRICHAT KAOWINN[1], CHUTIMA KAEWPIBOON[2], SANG SEOK KOH[3], OLIVER H. KRÄMER[4] and YOUNG-HWA CHUNG[1]

[1]BK21+, Department of Cogno-Mechatronics Engineering, Pusan National University, Busan 46241, Republic of Korea; [2]Department of Biology, Faculty of Science, Thaksin University, Phatthalung 93210, Thailand; [3]Department of Biological Sciences, Dong-A University, Busan 49315, Republic of Korea; [4]Department of Toxicology, University Medical Center Mainz, Mainz D-55131, Germany

Received December 27, 2017; Accepted September 3, 2018

DOI: 10.3892/or.2018.6701

Abstract. Our previous studies have shown that the novel oncogene, cancer upregulated gene 2 (CUG2), activates STAT1, which is linked to anticancer drug resistance, induces epithelial-mesenchymal transition (EMT) and cancer stem cell-like phenotypes as determined by MTT, migration and sphere formation assays. We thus aimed to ascertain whether the activation of STAT1 by CUG2 is involved in these malignant phenotypes besides drug resistance. Here, we showed that STAT1 suppression decreased the expression of N-cadherin and vimentin, biomarkers of EMT, which led to inhibition of the migration and invasion of human lung A549 cancer cells stably expressing CUG2, but did not recover E-cadherin expression. STAT1 siRNA also diminished CUG2-induced TGF-β signaling, which is critical in EMT, and TGF-β transcriptional activity. Conversely, inhibition of TGF-β signaling reduced phosphorylation of STAT1, indicating a crosstalk between STAT1 and TGF-β signaling. Furthermore, STAT1 silencing diminished sphere formation, which was supported by down-regulation of stemness-related factors such as Sox2, Oct4, and Nanog. Constitutive suppression of STAT1 also inhibited cell migration, invasion and sphere formation. As STAT1 acetylation counteracts STAT1 phosphorylation, acetylation of STAT1 by treatment with trichostatin A, an inhibitor of histone deacetylases (HDACs), reduced cell migration, invasion, and sphere formation. As HDAC4 is known to target STAT1, its role was investigated under CUG2 overexpression. HDAC4 suppression resulted in inhibition of cell migration, invasion, and sphere formation as HDAC4 silencing hindered TGF-β signaling and decreased expression of Sox2 and Nanog. Taken together, we suggest that STAT1-HDAC4 signaling induces malignant tumor features such as EMT and sphere formation in CUG2-overexpressing cancer cells.

Correspondence to: Professor Young-Hwa Chung, BK21+, Department of Cogno-Mechatronics Engineering, Pusan National University, Busan 46241, Republic of Korea
E-mail: younghc@pusan.ac.kr

Key words: CUG2, STAT1, HDAC4, epithelial-mesenchymal transition, sphere formation

Introduction

Cancer upregulated gene 2 (*CUG2*) has been identified as a candidate gene whose expression is commonly increased in various tumor tissues, including ovarian, liver, colon and lung, playing a crucial role in tumorigenesis (1). CUG2 has been identified as a new centromere component required for kinetochore function during cell division (2,3). The oncogenic effect of CUG2 was found to be similar to that of Ras in a transplant model using NIH3T3 cells (1). Although CUG2 overexpression activates Ras and mitogen-activated protein kinases (MAPKs), including p38 MAPK, which eventually facilitate oncolytic retroviral replication (4-6), CUG2 confers resistance to oncolytic vesicular stomatitis virus infection (7) and induces anticancer drug resistance through activation of STAT1 (8). Another study revealed that CUG2 induces epithelial-mesenchymal transition (EMT) through TGF-β signaling (9). Crosstalk between Sp1 and Smad2/3 mediated by CUG2 or TGF-β plays a crucial role during EMT (9).

Although the transcription factor STAT1 is well established as an important antiviral agent acting via IFN-associated intracellular signaling, the role of STAT1 in the development of cancer is still unclear: A tumor suppressor or oncogene? On the one hand, STAT1 functions as a tumor suppressor via the upregulation of caspases (10,11), cyclin-dependent kinase inhibitor 1A (Cdkn1a; also known as p21) (12), or the IFN-regulatory factor 1 (IRF1)/p53 pathway (13). On the other hand, a number of studies have indicated that in certain cellular contexts, the IFN/STAT1 signaling pathway may facilitate tumor cell growth (14,15). One study reported that resistance to ionizing radiation and IFNs are associated

with constitutive overactivity of the IFN/STAT1 pathway in radioresistant tumor cells (14). Other studies have also demonstrated that constitutive overexpression of STAT1 is positively correlated with the protection of tumor cells from genotoxic stress induced by doxorubicin (16) or cisplatin (17).

Histone deacetylases (HDACs) play important roles in the maintenance and function of chromatin by regulating the acetylation state of histones (18). Recent data suggest that HDACs regulate the acetylation state of many non-histone targets, including STAT1, MEF2A, and Foxo proteins (19-21). In particular, overexpression of HDAC4, belonging to the class IIa family of HDAC, is not only significantly associated with tumor size in malignant thyroid lesions (22), but also promotes tumor growth by suppressing p21 expression in colon (23), ovarian (24), and gastric (25) cancer cells. Therefore, HDAC4 has been suggested to be a useful diagnostic marker for prognosis of patients with cancer and a potential target for anticancer therapy.

Since CUG2 has been shown to induce EMT and cancer stem cell (CSC)-like phenotypes, this study aimed to explore whether activated STAT1 induced by CUG2 plays a crucial role in these malignant tumor features besides anticancer drug resistance. We report that the STAT1-HDAC4 signaling pathway, communicating with TGF-β signaling, contributes to the increase in cell migration, invasion, sphere formation, and expression of stemness-related factors in CUG2-overexpressing cancer cells.

Materials and methods

Cell cultures. Human lung cancer A549 cells (ATCC, Manassas, VA, USA) stably expressing the vector alone (A549-Vec) or CUG2 (A549-CUG2), and A549-CUG2 cells with stably silenced STAT1 (A549-CUG2-shSTAT1) or the control (A549-CUG2-shVec) were cultured in RPMI-1640 medium supplemented with 10% fetal bovine serum (FBS), 1% penicillin, 1% streptomycin, and G418 (0.5 mg/ml; Sigma-Aldrich; Merck KGaA, Darmstadt, Germany) at 37˚C with 5% CO_2. For A549-CUG2-shSTAT1 and A549-CUG2-shVec cells, puromycin (1 μg/ml; Sigma-Aldrich; Merck KGaA) was additionally added to the medium.

Reagents and antibodies. For immunoblotting, antibodies against STAT1 (#9172), phospho-STAT1 (#9171), Smad2/3 (#5678), and phospho-Smad2 (#3108) were acquired from Cell Signaling Technology (Danvers, MA, USA). Anti-β-actin (sc-4778), -Klf4 (sc-166229), -HDAC4 (sc-5245), and -Sp1 (sc-17824) antibodies were obtained from Santa Cruz Biotechnology (Santa Cruz, CA, USA) and antibodies against E-cadherin (ab15148), N-cadherin (ab18203), vimentin (ab137321), Snail (ab180714), Twist (ab175430), Bmi1 (ab126783), Sox2 (ab97959), and Oct4 (ab109183) were obtained from Abcam (Cambridge, MA, USA). LY2109761 and trichostatin A (TSA) were purchased from Cayman Chemical (Ann Arbor, MI, USA) and Sigma-Aldrich/Merck KGaA, respectively. The STAT1-shRNA vector was acquired from Origene (Rockville, MD, USA).

Cellular fractionation. Cells cultured in 100-mm plates were washed and harvested with ice-cold PBS, and cell pellets were lysed with 800 μl of TTN buffer [20 mM Tris-HCl (pH 7.4), 0.05% Triton X-100, 150 mM NaCl, 1 mM EDTA, 1 mM DTT, 10% glycerol, 0.5 mM PMSF, and 1X protease inhibitor cocktail] on ice for 20 min followed by centrifugation at 10,000 x g for 15 min. The supernatants represented the soluble fractions, and the pellets as insoluble fractions were subsequently solubilized in 800 μl of RIPA buffer [50 mM Tris-HCl (pH 7.4), 150 mM NaCl, 1 mM EDTA, 1 mM DTT, 1% NP-40, 0.5% deoxycholic acid, 0.1% SDS, 10% glycerol, 0.5 mM PMSF, and 1X protease inhibitor cocktail] on ice for 30 min and were centrifuged at 12,000 x g for 15 min. Thereafter, these supernatants were used as nuclear extracts.

Immunoblotting. Cells were harvested and lysed with lysis buffer containing 1% NP-40 and protease inhibitors (Sigma-Aldrich; Merck KGaA) for immunoblotting. Proteins from whole cell lysates were resolved by 8, 10, or 15% SDS-polyacrylamide gel electrophoresis (PAGE) and transferred onto nitrocellulose membranes. Primary antibodies were used at a 1:1,000 or 1:2,000 dilution, and secondary antibodies conjugated with horseradish peroxidase were used at a 1:2,000 dilution in 5% nonfat dry milk. After the final washing, the membranes were evaluated with an enhanced chemiluminescence reagent using Image Quant LAS 4000 Mini (GE Healthcare, Tokyo, Japan).

Luciferase reporter assay. A549-CUG2 cells were transfected with TGF-β promoter vectors (phTG5 and phTG7) (26) using Lipofectamine 2000 (Invitrogen; Thermo Fisher Scientific, Inc., Waltham, MA, USA). To normalize the transfection efficiency, a pGK-βgal vector that expresses β-galactosidase under the control of a phosphoglucokinase promoter was included in the transfection mixture. At 48 h post-transfection, cells were washed with cold PBS and lysed in a lysis solution [25 mM Tris (pH 7.8), 2 mM EDTA, 2 mM DTT, 10% glycerol, and 1% Triton X-100]. Luciferase activity was measured with a luminometer using a luciferase kit (Promega, Madison, WI, USA).

Short interfering RNA (siRNA) transfection. Cells were trypsinized and cultured overnight to achieve 60-70% confluence before siRNA transfection. Pre-made STAT1, HDAC4 (Bioneer, Daejeon, Korea), and a negative control siRNA (Bioneer) were mixed with Lipofectamine 2000. The cells were incubated with the transfection mixture for 6 h and then rinsed with medium containing 10% FBS. The cells were incubated for 40 h before harvesting.

Invasion assay. Invasion assays were performed using 48-well Boyden chambers (Neuroprobe, Gaithersburg, MD, USA). The lower wells of the chamber were filled with a standard culture medium. The chamber was assembled using polycarbonate filters (Neuroprobe) coated with Matrigel. Cells in a serum-free medium ($5x10^4$ cells/well) were seeded in the upper compartment of the chamber. After incubation for 24 h, cell migration was quantified by counting the number of migrated cells after staining with hematoxylin and eosin under a light microscope (Olympus, CKX31-11 PHP, Tokyo, Japan). The data shown are the mean values of three independent experiments.

Wound healing assay. Cell migration was assessed using a scratch wound assay. Briefly, cells were cultured in 12-well plates ($5x10^5$ cells/well). When the cells reached 90% confluence, a single wound was made in the center of the cell monolayer using a P-200 pipette tip. At 0, 12, and 24 h of incubation, the wound closure areas were visualized by light microscopy (Olympus) at a magnification of x100.

Cell adhesion assay. The wells in 96-well plates were coated with collagen I solution (100 μg/ml) at 4˚C for 12 h and were dried in a tissue-culture hood. Cells ($2x10^5$ cells/well) were seeded on the well and serum-free RPMI-1640 medium (100 μl) was added to the well. The cells were incubated at 37˚C for 30 min to allow the cells to adhere to the surface and thereafter the then any non-adherent cells in the well were washed off with the medium. After washing, the wells were furnished with medium containing 10% FBS and the adherent cells were incubated at 37˚C for 4 h. Thereafter, MTT assay was performed for cell counting as previously described (27).

Sphere formation assay. A549-CUG2 cells were transfected with siRNAs of STAT1, HDAC4, or the control. At 24 h post-transfection, the cells were collected and seeded in 24-well ultra-low attachment plates in a serum-free medium supplemented with 5 μg/ml insulin, 0.4% bovine serum albumin, 10 ng/ml basic fibroblast growth factor, and 20 ng/ml recombinant human epidermal growth factor for 2, 4 and 6 days. The size and number of spheroids were analyzed under a light microscope (Olympus). The criterion for sphere formation was set as spheroids larger than 50 μm in size. The data shown are the mean values of three independent experiments.

Immunofluorescence. Cells were fixed with 4% paraformaldehyde for 15 min, permeabilized with cold acetone for 15 min, blocked with 10% goat serum for 30 min, and incubated with primary antibodies (1:100 dilution) for 30 min at room temperature. After incubation, the cells were washed extensively with PBS, incubated with Alexa Fluor 418-conjugated goat anti-mouse or donkey anti-rabbit antibody (1:500 dilution; Molecular Probes, Eugene, OR, USA) in PBS for 30 min at room temperature, and washed 3 times with PBS. For nuclear staining, cells were incubated with DAPI for 5 min in the dark and washed 3 times with PBS. The stained cells were mounted using PBS containing 10% glycerol and photographed using a fluorescence microscope (Axio Observer D1; Zeiss, Oberkochen, Germany).

Statistical analysis. Data are presented as mean ± standard deviation (SD). One-way ANOVA or unpaired t-test was used for statistical analysis (GraphPad Prism 6; GraphPad Software, Inc., La Jolla, CA, USA). Data were considered statistically significant at the P-value <0.05.

Results

CUG2-mediated STAT1 activation increases cell migration and invasion. Since we reported that activation of STAT1 induced by CUG2 confers resistance to doxorubicin (8), we next explored whether STAT1 contributes to other malignant tumor features. Cell migration was observed after the center of the monolayer of A549-CUG2 cells treated with STAT1 siRNA or control siRNA was scratched. STAT1 siRNA inhibited cell migration compared with control siRNA (Fig. 1A). In addition, when A549-CUG2 cells treated with STAT1 siRNA were cultured in the upper chamber coated with Matrigel, the number of invaded cells in the lower chamber was lower than that treated with control siRNA, after staining with hematoxylin and eosin (Fig. 1B). Furthermore, we found that STAT1 siRNA-treated cells showed stronger attachment on collagen-coated wells compared with that of the control siRNA-treated cells, in a cell attachment assay (Fig. 1C). We also found that STAT1 silencing reduced expression of biomarkers of EMT, N-cadherin and vimentin, in A549-CUG2 cells (Fig. 1D). However, STAT1 suppression did not significantly recover E-cadherin expression in A549-CUG2 cells (Fig. 1D). Immunofluorescence assay showed that STAT1 silencing further reduced the intensity of vimentin staining (Fig. 1E) when compared with the control siRNA. These results suggest that activation of STAT1 induced by CUG2 is involved in EMT.

As our recent study showed that TGF-β signaling plays a critical role in CUG2-induced EMT (9), we aimed to ascertain whether STAT1 is involved in CUG2-induced TGF-β signaling, leading to EMT. To answer this question, we transfected A549-CUG2 cells with STAT1 siRNA or control siRNA and examined expression of TGF-β signaling-related molecules such as Smad2, Snail, and Twist. As shown in Fig. 1F, we found that STAT1 silencing reduced phosphorylation of Smad2 in the cytoplasm and expression of Snail and Twist in the nucleus. These results prompted us to investigate whether STAT1 could affect TGF-β production. To solve this question, TGF-β promoter luciferase vector (pTG5) was introduced (26). STAT1 siRNA reduced the luciferase activity of TGF-β compared to that with control siRNA in A549-CUG2 cells, whereas STAT1 siRNA and control siRNA treatment failed to reduce luciferase activity of TGF-β promoter lacking Sp1 binding sites (pTG7) (Fig. 1G). The result indicates that both STAT1 and Sp1 are involved in the synthesis of TGF-β, a critical mediator of EMT. Conversely, when we suppressed TGF-β signaling with LY2109761 and examined STAT1 activation, we found that CUG2-induced phosphorylation of STAT1 was reduced (Fig. 1H), indicating that there is a crosstalk between the TGF-β and STAT1 signaling pathways.

CUG2-mediated STAT1 activation increases stemness-related factor expression and sphere formation. Our recent study showed that CUG2 overexpression induced CSC-like features, including sphere formation and elevated expression of stemness-related factors such as Bmi1, Klf4, Oct4, Sox2 and Nanog (unpublished data). We thus explored whether activation of STAT1 mediated by CUG2 is involved in the induction of CSC-like phenotypes. To answer this question, we examined spheroid forming ability after the suppression of STAT1 expression. We found that STAT1 siRNA restricted the size and number of spheroids in A549-CUG2 cells compared to the size and number in the control siRNA cells (Fig. 2A). In addition, STAT1 silencing significantly reduced Sox2, Oct4, and Nanog protein levels but failed to decrease Klf4 expression (Fig. 2B). STAT1 suppression only marginally diminished Bmi1protein levels (Fig. 2B). These results suggest that STAT1 plays a role

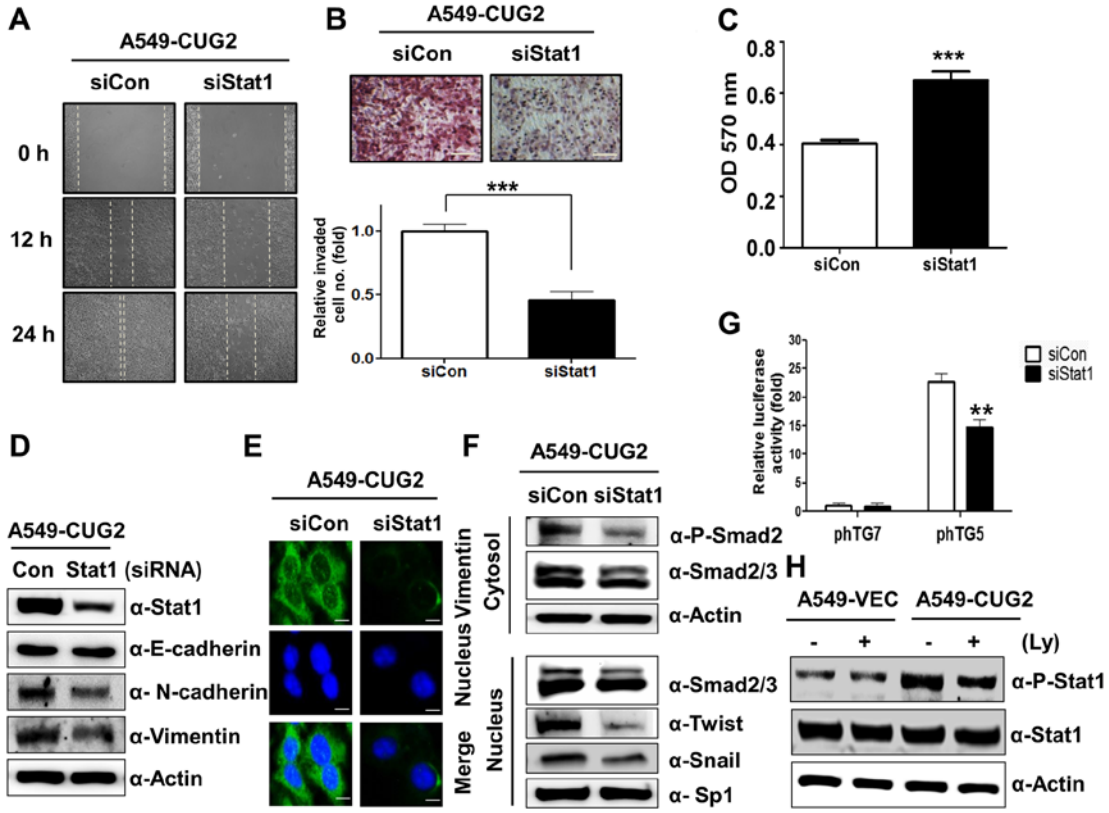

Figure 1. STAT1 silencing inhibits CUG2-induced cell migration and invasion. (A) Cell migration was measured by a wound healing assay at 48 h post-transfection with STAT1 siRNA (500 nM) or control siRNA. (B) An invasion assay was performed using 48-well Boyden chambers coated with Matrigel at 48 h post-transfection with STAT1 siRNA or control siRNA. Scale bar indicates 100 μm (***P<0.001). (C) At 48 h post-transfection with STAT1 siRNA or control siRNA, the A549-CUG2 cells were seeded in collagen-coated wells. The cells were incubated for 30 min for attachment and then the attached cells were analyzed by MTT assay (***P<0.001). (D and F) To examine an effect of STAT1 on levels of proteins related to EMT and TGF-β signaling, expression of STAT1, E-cadherin, N-cadherin, and vimentin was detected by immunoblotting at 48 h post-treatment with STAT1 siRNA or control siRNA. After transfection and cellular fractionation, expression of phospho-Smad2, Smad2/3, Snail, and Twist was detected by immunoblotting. (E) Expression of vimentin was detected by immunofluorescence using an Alexa Fluor 488-conjugated secondary antibody (green). DAPI was added for nuclear staining. Scale bar indicates 10 μm. (G) After A549-CUG2 cells treated with STAT1 siRNA or control siRNA were transfected with TGF-β promoter vectors (pTG5 and pTG7; 1 μg), luciferase enzyme activities were measured (**P<0.01). (H) A549-CUG2 cells were treated with LY2109761 (Ly; 10 μM) or DMSO for 24 h, and the cell lysates were prepared for immunoblotting to detect protein levels of phospho-STAT1 and STAT1.

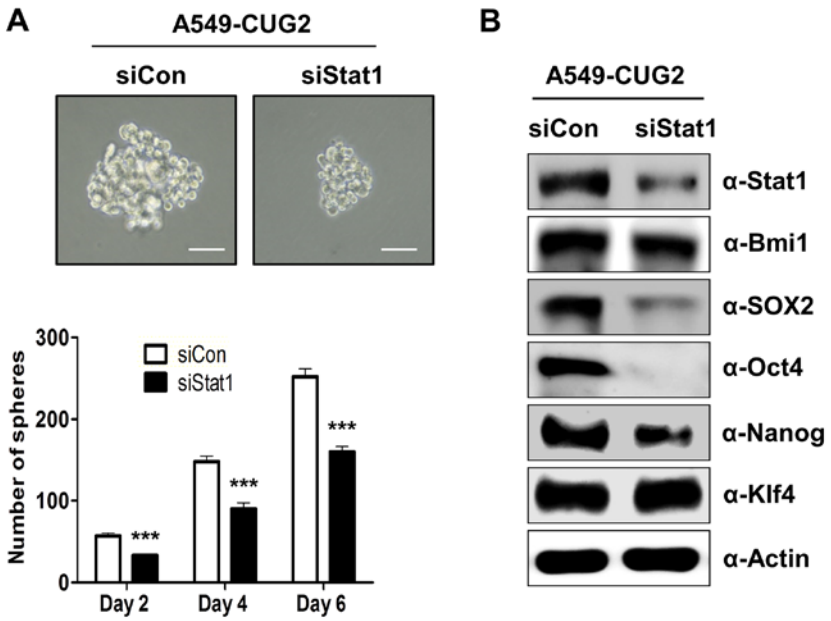

Figure 2. STAT1 silencing inhibits expression of stemness-related factors and sphere formation. (A) After transfection with STAT1 siRNA or control siRNA, spheroid size and number were evaluated at 2, 4 and 6 days post-seeding. A spheroid greater than 50 μm in size was the criterion for evaluating sphere formation. Scale bars indicate 50 μm (***P<0.001, compared to control siRNA). The assay was carried out from three independent experiments. (B) Expression of STAT1, Bmi1, Sox2, Oct4, Nanog and Klf4 was detected by immunoblotting at 48 h post-transfection with STAT1 siRNA or control siRNA.

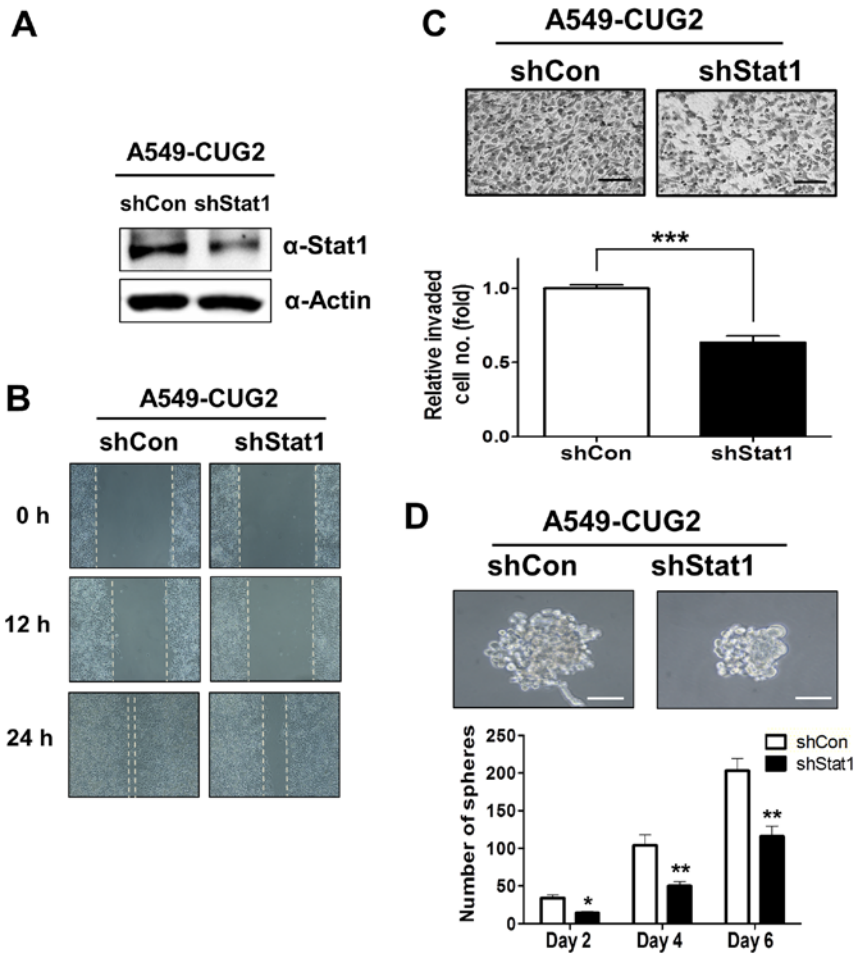

Figure 3. Constitutive suppression of STAT1 inhibits CUG2-induced cell migration, invasion, and sphere formation. (A) After transfection with sh-STAT1 (A549-CUG2-shSTAT1) or control plasmid (A549-CUG2-shVec) and selection under puromycin (1 μg/ml), suppression of STAT1 expression was confirmed by immunoblotting using an anti-STAT1 antibody. (B) After confluence of A549-CUG2-shSTAT1 and A549-CUG2-shVec cells, the cell monolayer was scratched. Cell migration was measured by a wound healing assay. (C) An invasion assay was compared between A549-CUG2-shSTAT1 and A549-CUG2-shVec cells using 48-well Boyden chambers coated with Matrigel. Scale bar indicates 100 μm (***P<0.001). (D) A549-CUG2-shSTAT1 and A549-CUG2-shVec cells were seeded in an ultra-low attachment 24-well plate. Spheroid size and number was evaluated at 2, 4 and 6 days post-seeding. Scale bars indicate 50 μm (*P<0.05, **P<0.01 compared to the A549-CUG2-shVec cells).

in sphere formation and expression of stemness-related factors such as Sox2, Oct4 and Nanog.

Constitutive suppression of STAT1 inhibits EMT and stemness in A549-CUG2 cells. Finally, to confirm the roles of STAT1 in biological features such as EMT and stemness, we constructed A549-CUG2 cells stably silencing STAT1 (A549-CUG2-shSTAT1) which was confirmed by immnoblotting (Fig. 3A). When cell migration was examined between A549-CUG2-shSTAT1 cells and the control (A549-CUG2-shVec) cells with wound-healing assay, A549-CUG2-shSTAT1 cells showed a slower migration rate than A549-CUG2-shVec cells (Fig. 3B). When cell invasion was examined between them, A549-CUG2-shSTAT1 cells significantly exhibited a reduced invasion in lower plate-wells compared to A549-CUG2-shVec cells (Fig. 3C). In addition, when we compared sphere forming ability between them, we found that A549-CUG2-shSTAT1 cells showed smaller size and a fewer number of spheroid than A549-CUG2-shVec cells (Fig. 3D). These results support that STAT1 is involved in EMT and stemness in A549 cell overexpressing CUG2.

HDAC4 is involved in the malignant tumor features of A549-CUG2 cells. As a recent study showed that activation of STAT1 is not only regulated by phosphorylation but also acetylation (28), we introduced TSA, an inhibitor of HDACs, in A549-CUG2 cells. Treatment with TSA inhibited cell migration and invasion compared to those with control DMSO treatment (Fig. 4A and B). In addition, treatment with TSA diminished the size and number of spheroids compared to that with DMSO treatment (Fig. 4C). These results indicate that STAT1 acetylation induced by inhibition of HDACs, a less active form of STAT1, exerts a negative influence on CUG2-mediated cell migration, invasion, and sphere formation.

Moreover, because STAT1 is a direct substrate of HDAC4 as a non-histone protein (21), we explored whether HDAC4 plays a role in CUG2-induced malignant tumor features such as rapid cell migration, aggressive invasion, and enhanced sphere formation. To answer this question, we suppressed HDAC4 expression using siRNA in A549-CUG2 cells and examined the malignant tumor features. Treatment with HDAC4 siRNA inhibited cell migration and invasion compared to control RNA treatment (Fig. 5A and B).

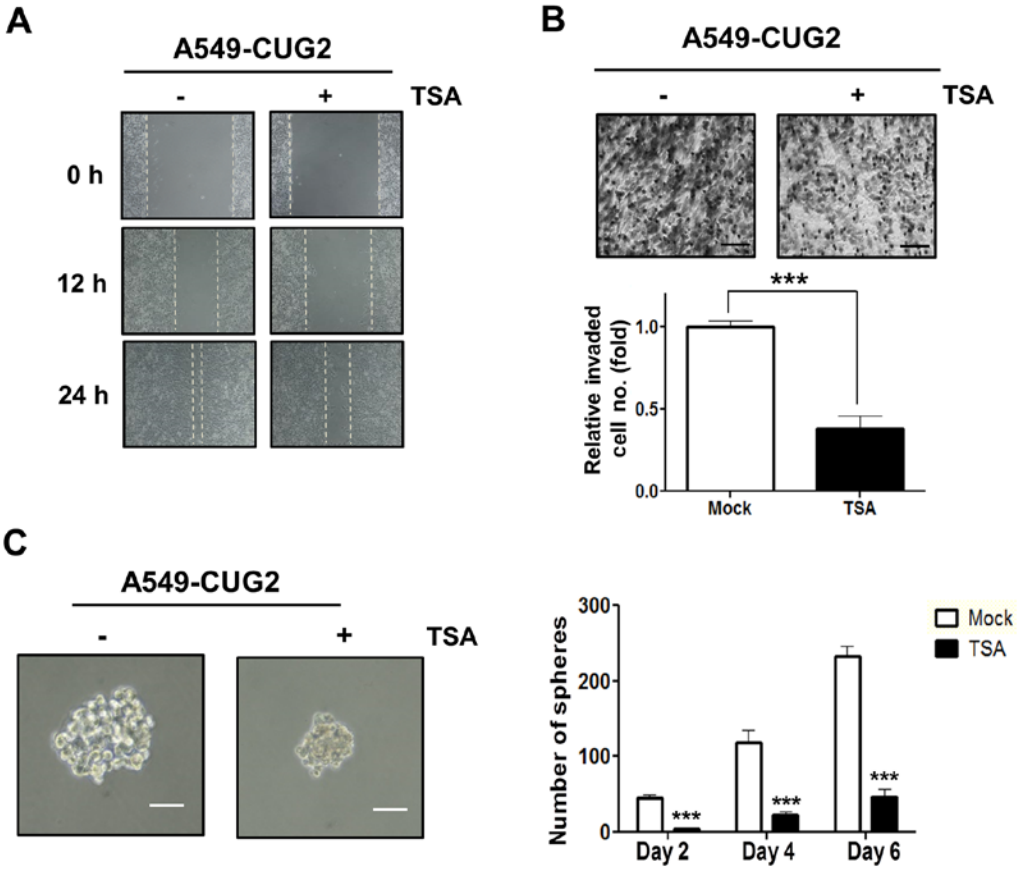

Figure 4. Treatment with TSA inhibits CUG2-induced cell migration, invasion and sphere formation. (A) A549-CUG2 cells were treated with TSA (100 nM) or DMSO for 24 h, and the cell monolayer was scratched. Cell migration was measured by a wound healing assay. (B) An invasion assay was performed after treatment with TSA or DMSO using 48-well Boyden chambers coated with Matrigel. Scale bar indicates 100 μm (***P<0.001). (C) After treatment with TSA (100 nM) or DMSO, the cells were seeded in an ultra-low attachment 24-well plate. Spheroid size and number was evaluated at 2, 4 and 6 days post-seeding. Scale bars indicate 50 μm (***P<0.001, compared to DMSO).

In addition, we found that HDAC4 siRNA-treated cells showed stronger attachment on the collagen-coated wells compared with that of control siRNA-treated cells, in a cell attachment assay (Fig. 5C). We also found that HDAC4 suppression inhibited expression of N-cadherin and vimentin but failed to recover E-cadherin expression as observed with STAT1 silencing (Fig. 5D). When we examined whether HDAC4 affected rapid cell migration and aggressive invasion through TGF-β signaling, we found that HDAC4 suppression decreased the phosphorylation level of Smad2 in the cytoplasm and expression of Snail and Twist in the nucleus (Fig. 5E). HDAC4 silencing also reduced the luciferase activity of the TGF-β promoter (Fig. 5F). These results suggest that HDAC4 is involved in EMT through TGF-β signaling in A549-CUG2 cells.

Furthermore, we also aimed to ascertain whether HDAC4 plays a role in CSC-like phenotypes, such as sphere formation and expression of stemness-related factors. HDAC4 silencing diminished the size and number of spheroids compared to that in the control (Fig. 6A). HDAC4 siRNA reduced expression of Sox2 and Nanog compared to that following control siRNA treatment but failed to decrease the expression of Bmi1, Oct4 and Klf4 (Fig. 6B). These results suggest that HDAC4 is involved in the sphere formation and increases Sox2 and Nanog expression in A549-CUG2 cells.

Discussion

Regarding a role of STAT1 in tumorigenesis, some studies have shown that STAT1 is activated during PDGF signaling (29). Indeed the studies reported that both enhanced STAT1 expression and activity occur exclusively in cells able to undergo EMT (29). In addition, another study showed that the EGFR-STAT1 axis participates in the metastasis of pancreatic cancer cells (30). These studies support our finding that activation of STAT1 under CUG2 overexpression plays a crucial role in EMT and CSC-like phenotypes. Furthermore, our recent study showed that TGF-β is also associated with these features induced by CUG2 (9) (unpublished data). As the underlying mechanism, we suggest that STAT1 might exert an influence on TGF-β signaling, which is critical for EMT, as we identified that STAT1 silencing not only inhibited Smad2 phosphorylation and Snail and Twist expression but also CUG2-induced TGF-β transcriptional activity. TGF-β signaling conversely affected STAT1 activation under CUG2 overexpression, suggesting a crosstalk between the TGF-β and STAT1 signaling pathways. However, the detailed mechanism will be investigated in our next study.

Interestingly, we found that STAT1 suppression inhibited CUG2-induced elevation of stemness-related factors, specifically Sox2 and Oct4, and Nanog, but not Klf4. Despite the

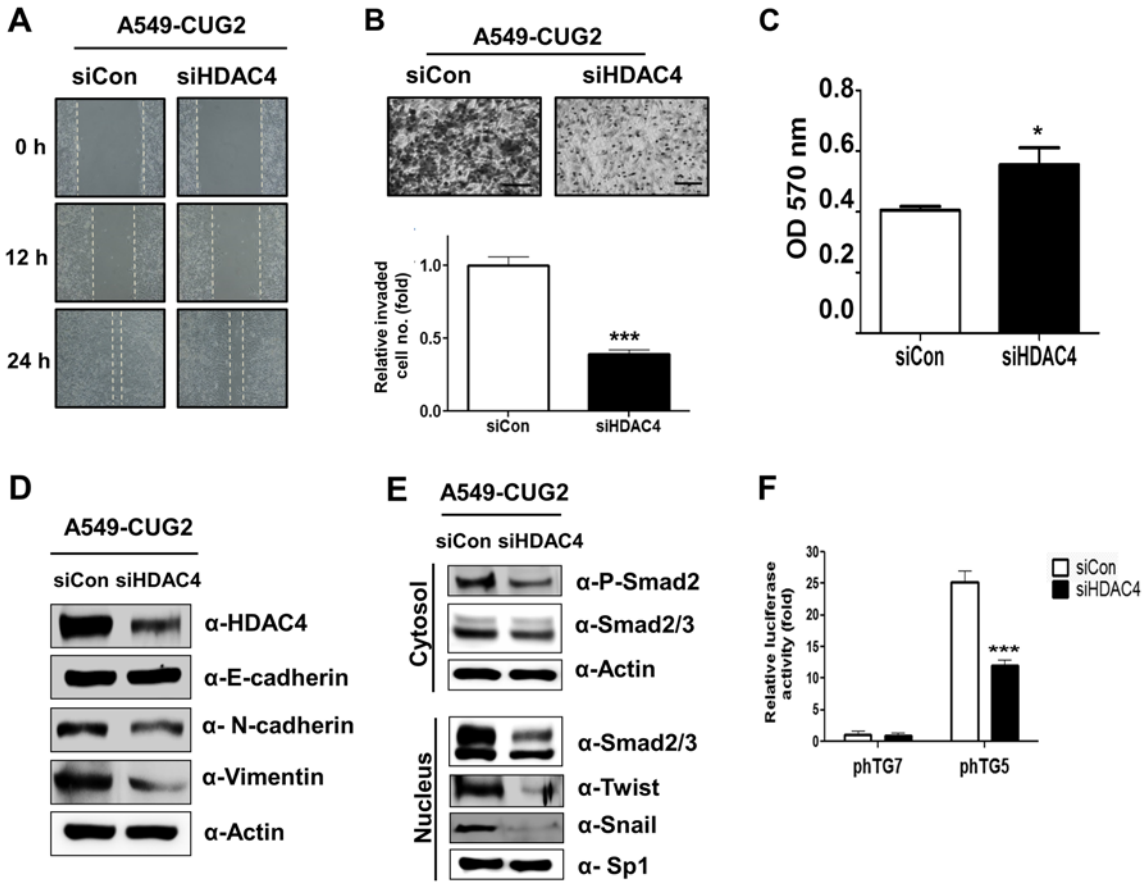

Figure 5. HDAC4 suppression reduces CUG2-induced cell migration and invasion. (A) Cell migration was measured by a wound healing assay at 48 h post-transfection with HDAC4 siRNA (500 nM) or control siRNA. (B) An invasion assay was performed after transfection with HDAC4 siRNA or control siRNA using 48-well Boyden chambers coated with Matrigel. Scale bar indicates 100 μm (***P<0.001, compared to control siRNA). (C) To examine an effect of HDAC4 on cell adhesion, A549-CUG2 cells were seeded in collagen-coated wells at 48 h post-transfection with HDAC4 siRNA or control siRNA. The cells were incubated for 30 min for attachment and then the number of the attached cells were analyzed by MTT assay (*P<0.05). (D) To examine an effect of HDAC4 on levels of proteins related to EMT, expression of HDAC4, E-cadherin, N-cadherin and vimentin was detected by immunoblotting at 48 h post-treatment with HDAC4 or control siRNAs. (E) To examine a role of HDAC4 in CUG2-induced upregulation of TGF-β signaling, expression of phospho-Smad2, Smad2/3, Snail, and Twist was detected by immunoblotting after transfection and cellular fractionation. (F) To examine a role of HDAC4 in CUG2-induced upregulation of TGF-β transcriptional activity, A549-CUG2 cells were transfected with TGF-β promoter vectors (pTG5, pTG7; 1 μg) at 12 h post-treatment with HDAC4 siRNA or control siRNA. Luciferase enzyme activities were then measured at 36 h post-transfection (***P<0.001, compared to control siRNA).

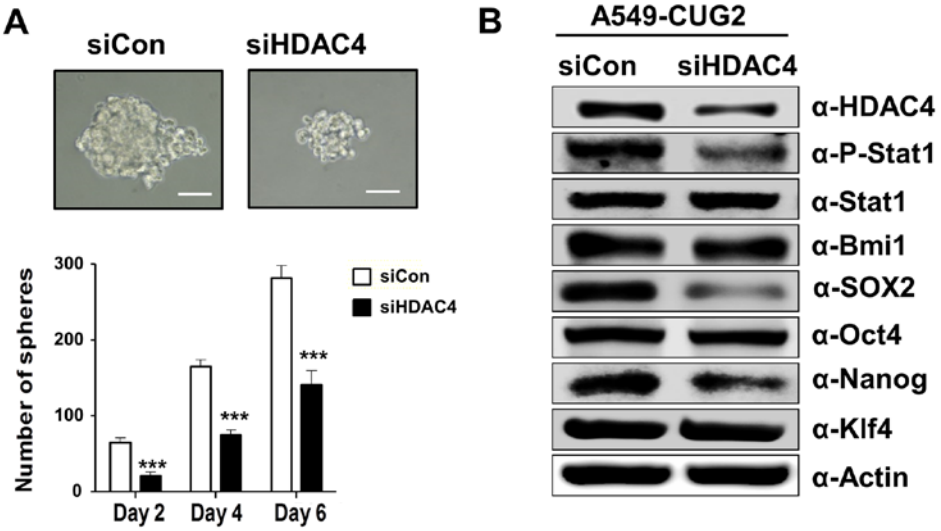

Figure 6. Suppression of HDAC4 impairs CUG2-induced sphere formation and expression of Sox2 and Nanog. (A) After treatment with HDAC4 siRNA or control siRNA, the cells were seeded in an ultra-low attachment 24-well plate. Spheroid size and number were evaluated at 2, 4 and 6 days post-seeding. Scale bars indicate 50 μm. The assay was carried out from three independent experiments. (***P<0.001, compared to control siRNA). (B) Expression of HDAC4, phosphorylated STAT1, STAT1, Bmi1, Sox2, Oct4, Nanog, and Klf4 was detected by immunoblotting at 48 h post-transfection with HDAC4 siRNA or control siRNA.

differential effect of STAT1 on stemness-related factors, we suggest that activated STAT1 could contribute to CUG2-induced CSC-like phenotypes. The relationship between STAT1 and stemness could be supported by the evidence that STAT1 inhibits transcription of Sonic Hedgehog, which is involved in the development of breast cancer stem cells (CSCs) when CD24 expression is suppressed (31).

Another study demonstrated that STAT1 is a direct substrate of HDAC4 and interacts with HDAC4 (21); thus, we focused on HDAC4, which has been suggested to be an oncogene owing to the elevated expression of HDAC4 that contributes to tumor growth by the stabilization of HIF-1α (19) and reduction of p21 transcription (23). A recent study reported that HDAC4 positively regulates EMT of esophageal carcinoma cells by increasing the expression of vimentin and decreasing the expression of E-cadherin (32). Other reports showed that HDAC4 inhibitors induce apoptosis through ER stress in myeloma cells (33) and cytotoxicity in chemoresistant cancer cells (34), suggesting HDAC4 inhibitors as potential therapeutic drugs against cancer. These lines of evidence support our finding that suppression of HDAC4 inhibits CUG2-induced EMT and sphere formation. Of note, we found that STAT1 knockdown reduces HDAC4 expression whereas HDAC4 silencing inhibits STAT1 phosphorylation (35). As other studies showed that STAT1 acetylation inhibited IFNg-induced STAT1 phosphorylation (36,37), suggesting that STAT1 acetylation regulates STAT1 signaling, we propose that enhanced STAT1 acetylation due to HDAC4 silencing may reduce STAT1 phosphorylation. Taken together, these reports indicate an interplay between HDAC4 and STAT1. Here, we report that activation of STAT1-HDAC4 signaling induced by CUG2 is involved in malignant tumor features such as EMT and CSC-like phenotypes.

Acknowledgements

Not applicable.

Funding

This study was supported by a 2-year Research Grant from Pusan National University.

Availability of data and materials

The datasets used the present study are available from the corresponding author upon reasonable request.

Authors' contributions

SK, OHK, and YHC conceived and designed the study. SK and CK performed the experiments and SSK was involved in data compilation and analysis. SK and YHC wrote the paper. All authors read and approved the manuscript and agree to be accountable for all aspects of the research in ensuring that the accuracy or integrity of any part of the work are appropriately investigated and resolved.

Ethics approval and consent to participate

Not applicable.

Patient consent for publication

Not applicable.

Competing interests

The authors declare no competing financial interest.

References

1. Lee S, Gang J, Jeon SB, Choo SH, Lee B, Kim YG, Lee YS, Jung J, Song SY and Koh SS: Molecular cloning and functional analysis of a novel oncogene, cancer-upregulated gene 2 (*CUG2*). Biochem Biophys Res Commun 360: 633-639, 2007.
2. Hori T, Amano M, Suzuki A, Backer CB, Welburn JP, Dong Y, McEwen BF, Shang WH, Suzuki E, Okawa K, *et al*: CCAN makes multiple contacts with centromeric DNA to provide distinct pathways to the outer kinetochore. Cell 135: 1039-1052, 2008.
3. Kim H, Lee M, Lee S, Park B, Koh W, Lee DJ, Lim DS and Lee S: Cancer-upregulated gene 2 (CUG2), a new component of centromere complex, is required for kinetochore function. Mol Cells 27: 697-701, 2009.
4. Park EH, Park EH, Cho IR, Srisuttee R, Min HJ, Oh MJ, Jeong YJ, Jhun BH, Johnston RN, Lee S, *et al*: CUG2, a novel oncogene confers reoviral replication through Ras and p38 signaling pathway. Cancer Gene Ther 17: 307-314, 2010.
5. McEntee G, Kyula JN, Mansfield D, Smith H, Wilkinson M, Gregory C, Roulstone V, Coffey M and Harrington KJ: Enhanced cytotoxicity of reovirus and radiotherapy in melanoma cells is mediated through increased viral replication and mitochondrial apoptotic signalling. Oncotarget 7: 48517-48532, 2016.
6. Sborov DW, Nuovo GJ, Stiff A, Mace T, Lesinski GB, Benson DM Jr, Efebera YA, Rosko AE, Pichiorri F, Grever MR, *et al*: A phase I trial of single-agent reolysin in patients with relapsed multiple myeloma. Clin Cancer Res 20: 5946-5955, 2014.
7. Malilas W, Koh SS, Srisuttee R, Boonying W, Cho IR, Jeong CS, Johnston RN and Chung YH: Cancer upregulated gene 2, a novel oncogene, confers resistance to oncolytic vesicular stomatitis virus through STAT1-OASL2 signaling. Cancer Gene Ther 20: 125-132, 2013.
8. Malilas W, Koh SS, Kim S, Srisuttee R, Cho IR, Moon J, Yoo HS, Oh S, Johnston RN and Chung YH: Cancer upregulated gene 2, a novel oncogene, enhances migration and drug resistance of colon cancer cells via STAT1 activation. Int J Oncol 43: 1111-1116, 2013.
9. Kaowinn S, Kim J, Lee J, Shin DH, Kang CD, Kim DK, Lee S, Kang MK, Koh SS, Kim SJ, *et al*: Cancer upregulated gene 2 induces epithelial-mesenchymal transition of human lung cancer cells via TGF-βeta signaling. Oncotarget 8: 5092-5110, 2017.
10. Chin YE, Kitagawa M, Kuida K, Flavell RA and Fu XY: Activation of the STAT signaling pathway can cause expression of caspase 1 and apoptosis. Mol Cell Biol 17: 5328-5337, 1997.
11. Kumar A, Commane M, Flickinger TW, Horvath CM and Stark GR: Defective TNF-alpha-induced apoptosis in STAT1-null cells due to low constitutive levels of caspases. Science 278: 1630-1632, 1997.
12. Chin YE, Kitagawa M, Su WC, You ZH, Iwamoto Y and Fu XY: Cell growth arrest and induction of cyclin-dependent kinase inhibitor $p21^{WAF1/CIP1}$ mediated by STAT1. Science 272: 719-722, 1996.
13. Townsend PA, Scarabelli TM, Davidson SM, Knight RA, Latchman DS and Stephanou A: STAT-1 interacts with p53 to enhance DNA damage-induced apoptosis. J Biol Chem 279: 5811-5820, 2004.
14. Khodarev NN, Beckett M, Labay E, Darga T, Roizman B and Weichselbaum RR: STAT1 is overexpressed in tumors selected for radioresistance and confers protection from radiation in transduced sensitive cells. Proc Natl Acad Sci USA 101: 1714-1719, 2004.
15. Weichselbaum RR, Ishwaran H, Yoon T, Nuyten DS, Baker SW, Khodarev N, Su AW, Shaikh AY, Roach P, Kreike B, *et al*: An interferon-related gene signature for DNA damage resistance is a predictive marker for chemotherapy and radiation for breast cancer. Proc Natl Acad Sci USA 105: 18490-18495, 2008.
16. Fryknas M, Dhar S, Oberg F, Rickardson L, Rydaker M, Goransson H, Gustafsson M, Pettersson U, Nygren P, Larsson R and Isaksson A: STAT1 signaling is associated with acquired crossresistance to doxorubicin and radiation in myeloma cell lines. Int J Cancer 120: 189-195, 2007.

17. Roberts D, Schick J, Conway S, Biade S, Laub PB, Stevenson JP, Hamilton TC, O'Dwyer PJ and Johnson SW: Identification of genes associated with platinum drug sensitivity and resistance in human ovarian cancer cells. Br J Cancer 92: 1149-1158, 2005.
18. Yang XJ and Seto E: HATs and HDACs: From structure, function and regulation to novel strategies for therapy and prevention. Oncogene 26: 5310-5318, 2007.
19. Geng H, Harvey CT, Pittsenbarger J, Liu Q, Beer TM, Xue C and Qian DZ: HDAC4 protein regulates HIF1α protein lysine acetylation and cancer cell response to hypoxia. J Biol Chem 286: 38095-38102, 2011.
20. Mihaylova MM, Vasquez DS, Ravnskjaer K, Denechaud PD, Yu RT, Alvarez JG, Downes M, Evans RM, Montminy M and Shaw RJ: Class IIa histone deacetylases are hormone-activated regulators of FOXO and mammalian glucose homeostasis. Cell 145: 607-621, 2011.
21. Stronach EA, Alfraidi A, Rama N, Datler C, Studd JB, Agarwal R, Guney TG, Gourley C, Hennessy BT, Mills GB, *et al*: HDAC4-regulated STAT1 activation mediates platinum resistance in ovarian cancer. Cancer Res 71: 4412-4422, 2011.
22. Giaginis C, Alexandrou P, Delladetsima I, Giannopoulou I, Patsouris E and Theocharis S: Clinical significance of histone deacetylase (HDAC)-1, HDAC-2, HDAC-4, and HDAC-6 expression in human malignant and benign thyroid lesions. Tumour Biol 35: 61-71, 2014.
23. Wilson AJ, Byun DS, Nasser S, Murray LB, Ayyanar K, Arango D, Figueroa M, Melnick A, Kao GD, Augenlicht LH and Mariadason JM: HDAC4 promotes growth of colon cancer cells via repression of p21. Mol Biol Cell 19: 4062-4075, 2008.
24. Shen YF, Wei AM, Kou Q, Zhu QY and Zhang L: Histone deacetylase 4 increases progressive epithelial ovarian cancer cells via repression of p21 on fibrillar collagen matrices. Oncol Rep 35: 948-954, 2016.
25. Kang ZH, Wang CY, Zhang WL, Zhang JT, Yuan CH, Zhao PW, Lin YY, Hong S, Li CY and Wang L: Histone deacetylase HDAC4 promotes gastric cancer SGC-7901 cells progression via p21 repression. PLoS One 9: e98894, 2014.
26. Kim SJ, Glick A, Sporn MB and Roberts AB: Characterization of the promoter region of the human transforming growth factor-beta 1 gene. J Biol Chem 264: 402-408, 1989.
27. Zhang Y, Wang W, Wang Y, Huang X, Zhang Z, Chen B, Xie W, Li S, Shen S and Peng B: NEK2 promotes hepatocellular carcinoma migration and invasion through modulation of the epithelial-mesenchymal transition. Oncol Rep 39: 1023-1033, 2018.
28. Kramer OH and Heinzel T: Phosphorylation-acetylation switch in the regulation of STAT1 signaling. Mol Cell Endocrinol 315: 40-48, 2010.
29. Jechlinger M, Sommer A, Moriggl R, Seither P, Kraut N, Capodiecci P, Donovan M, Cordon-Cardo C, Beug H and Grunert S: Autocrine PDGFR signaling promotes mammary cancer metastasis. J Clin Invest 116: 1561-1570, 2006.
30. Seshacharyulu P, Ponnusamy MP, Rachagani S, Lakshmanan I, Haridas D, Yan Y, Ganti AK and Batra SK: Targeting EGF-receptor(s)-STAT1 axis attenuates tumor growth and metastasis through downregulation of MUC4 mucin in human pancreatic cancer. Oncotarget 6: 5164-5181, 2015.
31. Suyama K, Onishi H, Imaizumi A, Shinkai K, Umebayashi M, Kubo M, Mizuuchi Y, Oda Y, Tanaka M, Nakamura M, *et al*: CD24 suppresses malignant phenotype by downregulation of SHH transcription through STAT1 inhibition in breast cancer cells. Cancer Lett 374: 44-53, 2016.
32. Zeng LS, Yang XZ, Wen YF, Mail SJ, Wang MH, Zhang MY, Zheng XF and Wang HY: Overexpressed HDAC4 is associated with poor survival and promotes tumor progression in esophageal carcinoma. Aging 8: 1236-1249, 2016.
33. Kikuchi S, Suzuki R, Ohguchi H, Yoshida Y, Lu D, Cottini F, Jakubikova J, Bianchi G, Harada T, Gorgun G, *et al*: Class IIa HDAC inhibition enhances ER stress-mediated cell death in multiple myeloma. Leukemia 29: 1918-1927, 2015.
34. Marek L, Hamacher A, Hansen FK, Kuna K, Gohlke H, Kassack MU and Kurz T: Histone deacetylase (HDAC) inhibitors with a novel connecting unit linker region reveal a selectivity profile for HDAC4 and HDAC5 with improved activity against chemoresistant cancer cells. J Med Chem 56: 427-436, 2013.
35. Kaowinn S, Jun SW, Kim CS, Shin DM, Hwang YH, Kim K, Shin B, Kaewpiboon C, Jeong HH, Koh SS, *et al*: Increased EGFR expression induced by a novel oncogene, CUG2, confers resistance to doxorubicin through Stat1-HDAC4 signaling. Cell Oncol 40: 549-561, 2017.
36. Kramer OH, Knauer SK, Greiner G, Jandt E, Reichardt S, Gührs KH, Stauber RH, Böhmer FD and Heinzel T: A phosphorylation-acetylation switch regulates STAT1 signaling. Genes Dev 23: 223-235, 2009.
37. Ginter T, Bier C, Knauer SK, Sughra K, Hildebrand D, Munz T, Liebe T, Heller R, Henke A, Stauber RH, *et al*: Histone deacetylase inhibitors block IFNγ-induced STAT1 phosphorylation. Cell Signal 24: 1453-1460, 2012.